Animal Science Papers and Reports vol. 43 (2025) no. 3, 347-366
DOI: 10.2478/aspr-2025-0024
Institute of Genetics and Animal Biotechnology
of the Polish Academy of Sciences, Jastrzębiec, Poland

Assessment of spatiotemporal development of cell lineages in the mouse blastocyst using bespoke cell neighbourhood analysis approaches

Roberto de la Fuente[1,2‡*], Jessica E. Forsyth[2,3,4]

[1] Department of Experimental Embryology, Institute of Genetics and Animal Biotechnology of the Polish Academy of Sciences, Jastrzębiec, 05-552 Magdalenka, Poland

[2] Division of Developmental Biology, Faculty of Biology, Medicine and Health, University of Manchester, Manchester, United Kingdom

[3] School of Mathematics, Alan Turing Building, University of Manchester, Manchester, United Kingdom

[4] Division of Population Health, School of Medicine and Population Health, University of Sheffield, Sheffield, United Kingdom

[‡] Current address: Department of Biology, Faculty of Sciences, Autonomous University of Madrid, Madrid, Spain

(Accepted May 26, 2025)

This work demonstrates the efficiency of the software IVEN (Internal Versus External Neighbourhood) in describing the dynamic changes in neighbourhoods of all cell lineages in the mammalian blastocyst. In the mouse model, the primitive endoderm (PrE)/epiblast (Epi) dichotomy is established during blastocyst formation, which results in a seemingly random distribution of cells from both lineages within the ICM ('salt and pepper' model). Nevertheless, differences in cell potency, plasticity and distribution suggest that specific cell traits, such as environment, might be defining the ultimate fate acquisition. We have tested the new functionalities in the latest IVEN version and its efficiency to explore the changes in cell distribution within cell lineages and sub-populations. For this purpose, we have developed pipelines that combine functionalities from the imaging software (IMARIS) with IVEN internal algorithms to provide an insight into the dynamic cell neighbourhood within the early blastocyst. IVEN returns detailed reconstructions and numerical arrays that can be interpreted to describe the evolution of cell neighbourhoods within and between lineages. Thus, we have been able

*Corresponding author: roberto.delafuente@uam.es

to identify specific subsets of cells within the TE and the ICM lineages depending on their relative position to the blastocyst cavity and revealed distinct neighbourhood features. IVEN analyses were essential to provide quantitative understanding of the intrinsic dynamics of the mouse blastocyst. Our approach demonstrates the accuracy of IVEN as a descriptive analytical tool and offers the possibility of applying it on to other systems to uncover differences between species.

KEYWORDS: blastocyst / neighbourhood / classification / distance / primitive endoderm / epiblast / cavity

Cleavage divisions during mouse early development generate a compacted morula with asymmetric outer cells that will differentiate into the trophectoderm (TE) [Sutherland *et al.* 1990, Yamanaka *et al.* 2006, Nishioka *et al.* 2009]. After the outer/inner cell polarization is achieved, small cavities are formed in between the inner cell mass (ICM) cells [Wiley 1984, Manejwala *et al.* 1989] that eventually coalesce into a single one [Borland *et al.* 1977, McLaren and Smith 1977, Schliffka *et al.* 2024]. This growing large cavity occupies the vast majority of the volume as it pushes the whole ICM to one pole of the otherwise hollow blastocyst around the third day of development (E3.5). During the 24-48h-window that follows morula compaction, the ICM cells differentiate into either primitive endoderm (PrE) or epiblast (Epi) lineages and segregate into two defined compartments [Chazaud *et al.* 2006, Plusa *et al.* 2008, Filimonow and de la Fuente 2022]. The PrE/Epi bifurcation is not merely a positional question, but it may serve clues on how the 3D disposition of single cells impacts signalling by a morphogen such as FGF4 [De Mot *et al.* 2016, Tosenberg *et al.* 2017, Saiz *et al.* 2020, Raina *et al.* 2021] and, more importantly, whether the particular history or parentage of each individual cell can explain their eventual fate in the ICM.

To date, several research lines on the topology of cells within the ICM have attempted to uncover positional cues to demonstrate a non-stochastic model for the definition of ICM cells as either PrE or Epi precursors. Different tools have been developed to tackle the identity of cells in the blastocyst: 'MINS' (*Modular Interactive Nuclear Segmentation*) - Lou *et al.* [2014]; single cell quantification study with 3-dimensional neighbourhood [Fischer *et al.* 2020]; 'insideOutside' [Strawbridge *et al.* 2023] and 'IVEN' (*Internal Versus External Neighbourhood*) - Forsyth *et al.* [2021]. Regardless of the mathematical basis for the development of these tools, all of them employ different approaches to categorize cells as inside or outside, starting from confocal microscopy images. Side-to-side comparisons have demonstrated the high performance of 'insideOutside' and IVEN on this task [Forsyth *et al*. 2021, Strawbridge *et al.* 2023]. Recent improvements to IVEN (version 2.1.0) now allow for more comprehensive analyses via the incorporation of additional cell-specific information along with IVEN-derived quantifications of cell neighbourhoods/environment. In addition to the highly descriptive value contributed by the measurement of distances within cell neighbourhoods, the combined use with source image analysis software provides undisputable cell identity classification into either PrE or Epi. Furthermore, a novel feature in the current IVEN version allows for the definition of cell position relative to the blastocyst cavity, both for the outside and the inside compartments.

By describing blastocyst development using the new version of IVEN with additional information from IMARIS analyses, we demonstrate the accuracy of the improved new version in discriminating individual cells within populations, which in turn allows to identify new features of specific cells within all blastocyst lineages. The pipeline employed here can be applied to any other system, provided imaging of a hollow structure can be performed. Thus, we demonstrate the ability of IVEN to characterize the structure under study, its value to contribute to the understanding of the blastocyst architecture, and its potential to provide a unique perspective to morphological analyses.

Material and methods

Embryo collection and culture

Embryos were obtained from mouse females during the third or the fourth day of embryonic development (E3.5 to E4.75, respectively), by flushing out the uterus directly into pre-warmed home-made manipulation medium M2 [Fulton and Whittingham 1978, Grabarek and Plusa 2012]. For proper *in vitro* culture, blastocysts were first removed their zonae pellucidae by treatment with acidic Tyrode's solution (Sigma Aldrich), according to previous protocols [Nicolson *et al.* 1975]. Blastocysts were cultured in home-made KSOM medium under mineral oil (Sigma Aldrich) in 35mm culture Petri dishes (Corning® Sigma Aldrich) at 37.5°C and 5% CO_2, and subsequently fixed in 4% paraformaldehyde (PFA) (Sigma Aldrich) in PBS (+0.01% Triton X-100 (Sigma Aldrich) + 0.1% Tween 20 (Sigma Aldrich)) for 20 minutes at room temperature before immunostaining protocols.

Mouse strains and husbandry

The mouse strains used for this study were CD1 (outbred from Jackson Laboratories) and F1 (C57Bl10 x CBA/H). All animals used were kept at the Animal Facility at the Institute of Genetics and Animal Biotechnology of the Polish Academy of Sciences (Jastrzębiec, Poland), under tight 12-hour light cycles, and fed *ad libitum*. Animal handling and experiments were conducted on the basis of the EU Directive 2010/63/EU of the European Parliament of the Council of 22nd September 2010 on the Protection of Animals Used for Scientific Purposes (OJ L 276, 20.10.2010, p.33), according to the Polish Governmental Act for Animal Care (Law from 15th January on the Protection of Animals Used for Scientific or Educational Purposes Act, Law Bulletin 266).

Immunodetection of proteins

The standard protocol for immunostaining of mouse embryos previously reported [Plusa *et al.* 2008] was consistently carried out for this study. After zona removal and blastocyst fixation (E4.0-E4.75 blastocysts were fixed straight away after collection because they had already hatched), a permeabilization step in 0.55% Triton X-100 in PBS was undertaken for 20 minutes to ensure antibody penetration into the embryo.

Incubation in 10% donkey serum (Sigma Aldrich) in PBS as a blocking buffer 1 hour at 4°C was performed before all antibody incubations. Immunostaining was achieved by incubating in a combination of the following primary antibodies: goat anti-GATA4 (sc1237) at a 1:300 dilution, mouse anti-SOX2 (ab79351) at 1:100, goat anti-SOX2 (AF2018) at 1:100, mouse anti-CDX2 (mu392A-UC) at 1:100, and mouse anti-CDX2 (BioGenex) at 1:1. Secondary antibodies (Alexa Fluor-conjugated from Invitrogen) were all applied at 1:500 for 1 hour at 4°C, and finally embryos were incubated in a 10 μM Hoechst 33342 (Molecular Probes) dilution in PBS + 0.1% Triton X-100 for 20 minutes to stain DNA.

Image and data analyses

Imaging of embryos was performed on a 35 mm glass-bottom Petri dish (Corning® Sigma Aldrich). Acquisition of 1 or 2 μm-thick sections in the Z axis for optical sectioning in the NIS-Elements software (Nikon Instruments Inc.) was done on a Nikon A1-R HD25 inverted confocal microscopes, and images were processed through IMARIS Cell 9.8 software (Bitplane, Oxford Instruments). Images after the staining protocol allow for the identification of cell nuclei in the Hoechst channel and defined lineages; cell centres were then marked using the 'Spot' generation option on IMARIS. This was followed by manual correction and appropriate labelling through the 'Classes' tool for cell lineage identification. Identified cell centres were then used to quantify fluorescence intensity signal within the volume of the 'spot' sphere, which allowed for normalization of the signal against Hoechst measured intensity, as performed previously [Forsyth *et al*. 2021]. Data compiled on IMARIS were exported as Excel workbooks and formatted accordingly by the application of in-house built macros for its use on IVEN 2.1.0.

Statistical inference

Data preparation and curation were done on Excel 365, and all statistical tests and graph generation were performed on GraphPad Prism 9.5.1 (GraphPad Software, LLC). Analyses of cell neighbourhood as defined previously included assessment of distribution of outer cells around inside cells, i.e., how many TE cells –outside neighbours– are in the immediate surroundings of each cell within the ICM –inside neighbours), and how such cell microenvironment evolves over blastocyst development. Differences were addressed between inside and outside lineages, as well as within ICM lineages. Lineage packing or compaction as a developmental feature [Plusa *et al.* 2008, Forsyth *et al*. 2021, Filimonow and de la Fuente 2022] is suitable of study by measuring distances between cells both between and within lineages. Quantification of neighbouring cells and distances between them are direct outputs from the IVEN software [Forsyth *et al*. 2021].

Identification of specific groups of cells is a task result of the combination of features from Imaris and IVEN, which let us select any number of cells from any lineage with any feature of interest. Differences in cell position within the ICM relative to the blastocyst cavity and the possible correlation with protein levels were addressed

by the comparison of intensity of fluorescent signal between subpopulations of cells. Identification of said subsets was possible by applying filters created on Imaris to the output Excel files generated by IVEN. This methodology allowed to identify and pinpoint individual cells for any analysis required.

All graphs show mean and standard deviation (SD) as error bars, unless otherwise stated. Normal distribution of data was checked by the Anderson-Darling and by Shapiro-Wilk tests, according to sample size. For 2-group comparisons, the Student *t*-test was used for two sets of normally-distributed data; otherwise, non-parametric Mann-Whitney was performed. Regular one-way ANOVA plus Welch's test was performed as a parametric test, whereas the Kruskal-Wallis test was applied for non-parametric tests (plus multiple sample comparisons). Figures were built from original IVEN output images, through combined processing using IMARIS (Bitplane), ImageJ/FIJI 1.54 (from http://imagej.net) and GNU Image Manipulation Program (GIMP) 2.10.38.

IVEN analyses

Neighbourhood description was performed following the principles described previously [Forsyth *et al.* 2021]. The current IVEN v2.1.0 is available at https://github.com/jessforsyth/IVEN-code and includes updates to the following features: flexible data import, improvement of cell classification graphical user interface (GUI) with ability to display imported cell properties, classification of cavity-adjacent cells, and output of neighbour-to-neighbour distances. The updated IVEN version is supported in Python 3 and is thus freely available to all users.

Results and discussion

Outside/inside classification

The current IVEN v2.1.0 is the result of a Python implementation on the original version [Forsyth *et al.* 2021] that requires now a simpler data import structure, with only one header and four mandatory columns (additional optional properties can expand unlimitedly within the Excel spreadsheet). The first task to be performed by IVEN at any given stage of development is a 'routine' classification of outside/inside cells via the convex hull algorithm [Forsyth *et al.* 2021]. Should blastocysts be immunostained with antibodies against lineage-specific markers, manual correction following IVEN classification is possible (even though IVEN has been shown capable of accurately classifying the outside cells with minimal correction [Forsyth *et al.* 2021]). For instance, immunolocalization of CDX2, component of the Hippo pathway and typical marker of the TE [Niwa *et al.* 2005, Strumpf *et al.* 2005], allows for the visible discrimination between this lineage and the ICM in the cavitating early blastocyst (Fig. 1A.i). Confirmation of IVEN's account for the characterization of each cell neighbourhood in this case is straightforward; as seen in Forsyth *et al*. [2021], typically outside cells have more outside cell neighbours, whereas inside cells display a higher number of inside neighbours ($p<0.0001$) (Fig. 1A.ii-iv). The simultaneous use of antibodies against the

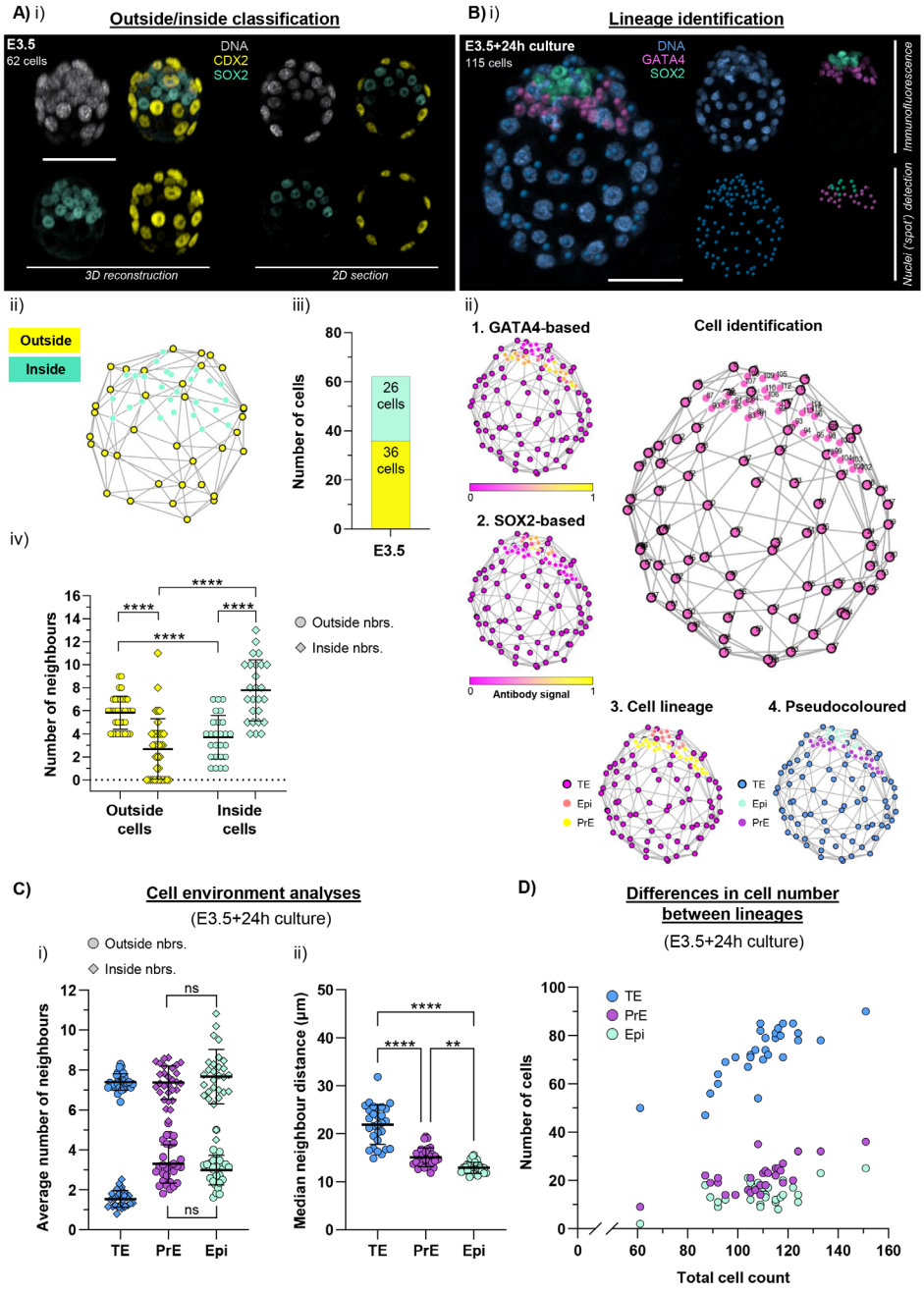
A) i)
Outside/inside classification
E3.5
62 cells
DNA
CDX2
SOX2
3D reconstruction
2D section
B) i)
Lineage identification
E3.5+24h culture
115 cells
DNA
GATA4
SOX2
Immunofluorescence
Nuclei ('spot') detection
ii)
Outside
Inside
iii)
Number of cells
26 cells
36 cells
E3.5
iv)
Number of neighbours
Outside cells
Inside cells
Outside nbrs.
Inside nbrs.
ii)
1. GATA4-based
2. SOX2-based
Antibody signal
Cell identification
3. Cell lineage
4. Pseudocoloured
TE
Epi
PrE
C)
Cell environment analyses
(E3.5+24h culture)
i)
Average number of neighbours
ns
TE
PrE
Epi
ii)
Median neighbour distance (µm)
D)
Differences in cell number between lineages
(E3.5+24h culture)
Number of cells
Total cell count

Fig. 1. Combination of IMARIS and IVEN's features for the description of neighbourhoods for each specific lineage in the mouse blastocyst. A) i) E3.5 blastocyst in which outside cells can be distinguished from inside cells by immunostaining for CDX2 and SOX2, respectively. ii) Matching IVEN classification of the same blastocyst, pseudocoloured, displaying the reconstruction from IMARIS labelling ('Outside' versus 'Inside'). iii) Cell count for each lineage of the blastocyst is shown, along with iv) their respective neighbourhood composition (outside vs inside neighbours). Differences are clearly displayed between lineages ($p<0.0001$). B) i) 3D view of a blastocyst collected at E3.5 and cultured in vitro for 24h that includes 'spot detection' for every cell nucleus on IMARIS. Spots are ascribed any identity required (e.g., cell lineage), so that the output file adds to IVEN classification. Immunostaining for PrE (GATA4) and Epi (SOX2) lineages allows to discriminate ICM lineages and subsequent confirmation of IVEN performance, if needed. Scale bars=50 μm. ii) IVEN reconstruction of the immunostained blastocyst in which identification of every individual cell is displayed (large). Small representations show how IVEN displays different lineages based on the antibody signal intensity (1 and 2), or on the interpretation of previous lineage tagging on IMARIS (3). Pseudocoloured panel (4) to match colours with the image from immunostaining. C) Assessment of neighbourhoods for the group of analyzed blastocysts (n=29). i) Neighbourhood composition, in average numbers for both outside and inside neighbours. No difference between lineages found with this regard at this stage: the PrE was calculated to present 3.29±0.96 outside neighbours, whereas the for the Epi this value was 2.98±0.74 ($p=0.4193$); similarly, 7.37±0.83 inside neighbours were calculated for the PrEn and 7.67±1.37 for the Epi ($p=0.4328$). ii) Distances (median) between neighbours for each lineage. D) Cell number for each lineage in blastocysts at different stages of development in vitro according to the total cell count (n=29 blastocysts).

PrE and Epi reinforces IVEN's performance on the correct classification of all lineages in the blastocyst (Fig. 1B.i). Information from image analysis software such as IMARIS, including binary cell fate allocation or protein expression levels, can be easily displayed within the IVEN interface to assist neighbourhood analyses (Fig. 1B.ii).

With the purpose of assessing how much the combination of IMARIS assessments and IVEN analyses allows for the quantification of spatial information for all different lineages within the early embryo, we analyzed E3.5 blastocysts cultured for an additional 24-hour-period. At a glance, the comparison of neighbourhood compositions between PrE (GATA4-positive) and Epi (SOX2-positive) cells within the cultured E3.5 embryos does not show statistically significant differences regarding the number of inside neighbours ($p=0.4328$) or outside ones ($p=0.4193$). However, higher values in the wider distribution for the Epi are indicative of the organization of these cells in the ICM (Fig. 1C.i). Segregation of PrE and Epi compartments is known to commence *in utero* at E3.75 stage (before the blastocyst reaches 100 cells) - Forsyth *et al.* [2021] and Yanagida *et al.* [2022]. Consequently, considering we did not find differences in neighbourhood composition between PrE and Epi at this moment, the data presented reveal that cells from both lineages still keep their 'salt and pepper' distribution, although some degree of segregation has already been achieved during the *in vitro* culture. This observation could be an explanation for the small but significant differences in distances between neighbours observed when comparing both ICM lineages ($p=0.0028$) (Fig. 1C.ii). The range of total cell number for the analyzed blastocysts (Fig. 1D) confirms the temporal window for PrE/Epi segregation, and indicates that this process is still ongoing in some of the E3.5 cultured embryos (Fig. 1D).

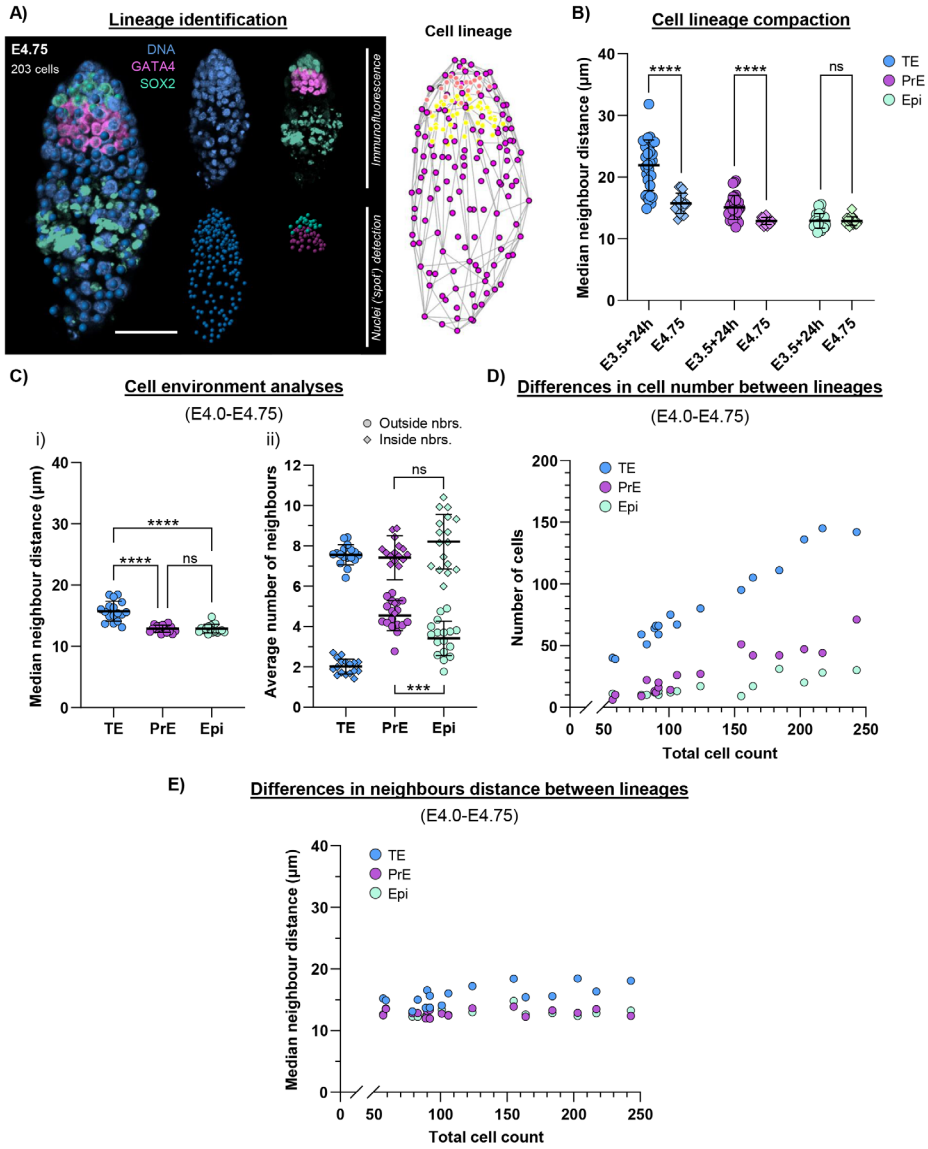

Fig. 2. Description of neighbourhoods for each lineage in peri-implantation mouse embryos. A) E4.75 peri-implantation blastocyst immunostained for GATA4 and SOX2. Previous spot detection and tagging into classes pave the way to interpret IVEN output data into information for each specific cell lineage. Scale bar=50 µm. B) Comparison of neighbour distances in each lineage between E3.5 blastocysts cultured in vitro for 24h and peri-implantation blastocysts collected at E4.75 reveals differences in cell organization in extra-embryonic lineages ($p<0.0001$ for comparisons of both TE and PrE). C) Detailed analyses of neighbourhood for all three lineages. i) Higher packing of cells in both ICM compartments

than in the TE is noticeable given the shorter distance between neighbours ($p<0.0001$ in both cases). ii) Differences in numbers of both outside and inside neighbours between PrE and Epi cells reflect their organization within the ICM. D) Cell number per lineage according to developmental stage of collected embryos based on their total cell count. E) Illustration of differences in distances between neighbours for every lineage over development of blastocysts. Note differences between TE and ICM are less accused than in the case of in vitro-cultured blastocysts shown previously (n=17 E4.0-E4.75 blastocysts).

Characterization of cell neighbourhoods

The distances between the centres of each neighbour ('cell centres') in absolute values is part of IVEN's output [Forsyth *et al.* 2021], which allows for the analysis of cell packing or compaction within their own compartment. In order to characterize the dynamics of each lineage during blastocyst maturation, we have also analyzed peri-implantation blastocysts (collected between E4.0 and E4.75) using IVEN to compare to the E3.5 cultured embryos (Fig. 2A). Our results resemble those previously described regarding the overall larger distances between cell centres in the TE than in the ICM lineages [Forsyth *et al.* 2021] - Figure 2B,C. We have also identified statistically significant differences in the median neighbour distances specifically in the PrE lineage between blastocysts at the two different developmental stages assessed ($p<0.0001$), which had not been described previously. Epi cells, in turn, did not show differences in compaction (distance between neighbours) between both stages ($p=0.8219$).

Both Epi and PrE mature during the expansion of the blastocyst cavity [Chazaud *et al.* 2006, Plusa *et al.* 2008, Saiz *et al.* 2013, 2016, Filimonow and de la Fuente 2022]. Once they have fully segregated from each other, their constituent cells exhibit even shorter distances between neighbours within each compartment, as demonstrated by the analysis of E4.75 peri-implantation blastocysts (Fig. 2B,C). After implantation is triggered, physical interactions with the endometrium cause warping and elongation of the early embryo, which alters its native shape. Despite this complex change in morphology, IVEN's quantification of the neighbourhood components seemingly remains robust and reliable; our analysis on freshly collected peri-implantation blastocysts highlights the increased packing of both ICM lineages when compared to the TE ($p<0.0001$ for both TE-PrE and TE-Epi) (Fig. 2C.i). Nevertheless, it also suggests an overall difference in cell-to-cell distances in both the TE (as previously demonstrated) and the PrE within cultured embryos (Fig. 2B). Contrary to the earlier stage assessed above, outer neighbourhood distribution in the Epi does differ significantly from that of the PrE ($p=0.0003$), illustrating that cells from the former lineage are mostly embedded in the inside of the ICM by the time of implantation (Fig. 2C.ii).

Integration of the Boolean output of outside/inside cells from IVEN into the analyses illustrates the inter-lineage differences on cell arrangement (compaction) and explains specific processes of blastocyst growth. Concomitant with the expansion of the cavity, the Epi and PrE lineages undergo specification and segregation into two different compartments in the ICM, while the integrity of the epithelial layer facing the cavity is maintained [Chazaud *et al.* 2006, Plusa *et al.* 2008]. The serial comparison of *in vitro*-

developing blastocysts by IVEN shows the tendency of the early embryo to compact the ICM lineages until certain developmental stage is reached. Up to around the 150-cell stage, TE cells grow in number simultaneously with the expansion of the cavity (more noticeable in *in vitro*-cultured blastocysts). Although the mural TE (mTE) proliferates more than the polar TE (pTE) - Copp [1978], Christodoulou *et al.* [2019], cavity growth causes a characteristic flattened shape of the TE cells adjacent to it (cavity-adjacent TE cells, here referred to as 'cTE'). Stretching of these cells thus causes distances between their centres to be longer than for the inside cells, mirroring what has been observed in the quantification of the neighbourhood by IVEN. From the 150-cell stage onwards, TE cell proliferation is quicker than cavity expansion (and than proliferation of ICM lineages) (Fig. 2D) and the blastocyst increases in cell number with no significant growth in size. Concomitantly, the ICM lineages also appear to be more tightly packed as the blastocyst approaches implantation. All these facts are reflected in the reduced distance between cell centres in all lineages quantified by the IVEN pipeline (Fig. 2C-E) and, as previously reported, explained by the decreasing cell diameter during cleavage divisions up to around E4.5 [Forsyth *et al.* 2021].

Definition of cavity-adjacent outside cells

In addition to the characterization of the environment within the blastocyst, a new feature allows IVEN to outline the blastocyst cavity and to define its limiting cells. The original version of the software was already able to discriminate between pTE and mTE considering the number of inside neighbours exhibited by outside cells [Forsyth *et al.* 2021], but the update to the software now enables the classification of cells along the internal boundary of the ICM. After the first outside/inside classification, the user is prompted to tag those cells that IVEN will employ to delineate the whole blastocyst cavity (Fig. 3A); such tagged cells are used to identify average points which should be located within the cavity centre. The main caveat the user may encounter during this procedure is the need to manually select a minimum number of partial cavities (named just 'cavities' in IVEN) to ensure all cells of interest are considered as or within the limits of the cavity. Despite the fairly regular spherical shape of cultured blastocysts, the identification of too few cavities may result in cell points left 'outside' the defined final cavity (both from the TE or from the ICM), leading to a misclassification in the output file for those particular cell spots (Fig. 3B). Although IVEN also allows for manual correction at this step, the optimal approach for the user in order to refine the outlined limits of the potential blastocyst cavity is to initially select enough cell spots to define several cavities. By so doing, IVEN accounts for all of them and returns a properly-defined cavity with all limiting cells correctly classified (Fig. 3B).

To test IVEN's accuracy in classifying cavity-adjacent cells, we first compared the results of the new feature with the ability to discriminate pTE and mTE based on their respective neighbourhoods in blastocysts collected at E3.5 and cultured *in vitro* for additional 24h. Our results showed a clear difference in the percentage of TE cells from each blastocyst identified as adjacent to the cavity, depending on whether this

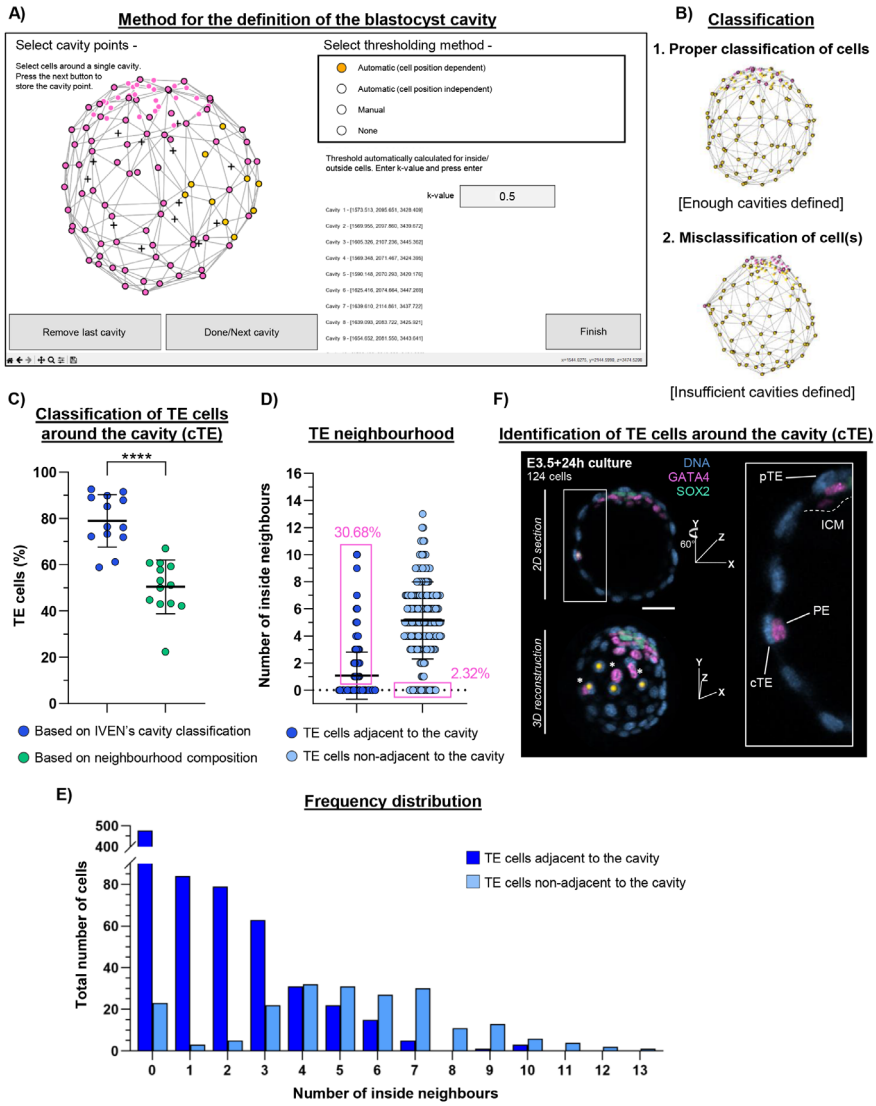

Fig. 3. Classification of cavity-adjacent cells in the TE. A) IVEN's interactive interface to select reference cavity-limiting cells sets the grounds for the definition of the cavity. Markers with black edges indicate outside cells as classified within the IVEN software, yellow points indicate selected points and black crosses are user-defined cavity points determined through averaging of manually selected cells. **B)** Results of cavity definition: all cells around the cavity are considered (1), or at least one TE cell is left outside the cavity when too few cavities are established (2). **C)** Percentage of TE cells (per blastocyst) defined as surrounding the cavity (cavity-adjacent TE cells – cTE) based on: IVEN's new cavity classification feature (blue), or on the presence/absence of inside neighbours (green). **D)** An average of 30.68±6.26% of TE cells per blastocyst are identified as being in contact with the cavity – cTE – even though they exhibit inside neighbours (dark blue), whereas a smaller fraction of them (2.32±3.29%) are

classified as belonging to the pTE domain, and yet show no inside neighbours (light blue) (cell fractions highlighted in pink). **E)** Frequency distribution of TE cells that show specific numbers of inside neighbours from the classification in (D). High numbers of them are still scarce among cells classified as cTE (dark blue). **F)** Immunostaining of an E3.5+24h blastocyst against GATA4 and SOX2. The inset highlights the presence of a PE cell (identified by its GATA4 signal) (gray spot) that was migrating over the inside side of the TE. 3D view of the same blastocyst rotated 60° in the Y axis to show cTE cells (yellow spots) in close proximity to migrating PE cells (asterisks) (inside neighbours of those cTE cells). **pTE**=polar TE, **ICM**=Inner cell mass, **PE**=parietal endoderm, **cTE**=cavity-adjacent TE. Scale bar=50 μm.

Table 1. Accuracy of classification of TE cells as either adjacent or non-adjacent to the blastocyst cavity varies when based on IVEN's specific cavity-defining feature *vs* when based on number of inside neighbours

Blastocysts (n)	Total cell count	Total TE cells	Total cTE cells identified by cavity analysis (% of TE cells per blastocyst)	Total cTE cells identified by inside neighbours=0 (% of TE cells per blastocyst)	Total non-matching cTE and mTE cells (% of TE cells per blastocyst)	Total non-matching non-cTE and pTE cells (% of TE cells per blastocyst)
13	1466	991	781 (78.81%±11.34%)	500 (50.45%±11.63%)	304 (30.68%±6.26%)	23 (2.32%±3.29%)

Number of TE cells from the set of analyzed blastocysts classified as adjacent to the cavity (cTE), based on the two different methods: IVEN's cavity and number of inside neighbours. Results of classification are shown as the portion of all TE cells, plus the average proportion (%) of cells per blastocysts ±SD. Data displayed in Fig. 3C,D. Mann-Whitney tests for comparison of two non-normally-distributed independent groups were run.

classification was based on IVEN's cavity definition feature (78.81%±11.34% of TE cells) or on the analysis of neighbourhoods (50.45%±11.63% of TE cells) ($p<0.0001$) - Table 1, and Figure 3C. Even if a given TE cell centre (spot) is located adjacent to the cavity, the cytoplasm of that particular TE cell can be in fact in physical contact with the ICM (meaning in close proximity to each other). In those cases, the cavity classification feature would classify such TE cells as pTE instead of mTE because of the presence of ICM cells in their neighbourhood (i.e., inside neighbours). To account for this difference, we quantified the proportion of potentially 'misclassified cells' based on the number of inside neighbours for every TE cell. Considering the total number of TE cells classified, on average 30.68% (±6.26%) of them per blastocysts were identified to be adjacent to the cavity (cTE cells by definition), despite exhibiting at least 1 inside neighbour (Tab. 1 and Fig. 3D,E). Similarly, though less likely, some TE cells might potentially be ascribed to the pTE group based on the cell centre position while having no inside neighbours, which would effectively define them as mTE cells. We detected that only 2.32% (±3.29%) of TE cells per blastocyst were classified in this way (Fig. 3D,E). This extremely high SD relative to the average value illustrates the variation between blastocysts, because this type of misclassified TE cells constitutes such an uncommon event.

A minimal amount of cTE cells were found to exhibit an unusually high number of inside neighbours (13, 6, 4, 2 and 1 cells displaying 9, 10, 11, 12 and 13 inside neighbours, respectively) (Fig. 3D,E). Because the histogram of frequency of inside neighbours for cTE cells shows a clear positively skewed distribution (Fig. 3E), we attributed this result to misclassification by IVEN, aware that the approach is not 100% perfect, and yet it provides a highly accurate discrimination between cavity-adjacent/non-adjacent cells.

In E4.5 blastocysts developing *in utero*, several PrE-derived cells are already detected as parietal endoderm (PE) cells in migration over the cavity face of the TE through a process that resembles epithelial-to-mesenchymal transition (EMT) [Veltmaat *et al.* 2000, Filimonow *et al.* 2019, Filimonow and de la Fuente 2022]. Whereas *in vitro*-cultured blastocysts do not show this feature in a prominent manner, some PrE/PE cells do occasionally exhibit migratory behavior (Fig. 3F). The position of such cells is then further away from the ICM surface, entirely in the cavity. Surrounding TE cells would then count on actual inside cells in their neighbourhood (thus being defined as cTE rather than mTE). This is fundamental to be accounted for when understanding the identity and architecture of the peri-implantation blastocyst. In our results, a large proportion of those cells originally regarded as 'misclassified' have few inside neighbours, which match the existence of migrating PE cells and the proximity of those cTE cells to the ICM (in contact with the so-called 'transition zone' - Filimonow and de la Fuente [2022]). Then again, in these more complex architectures, seemingly anomalous cells can be easily identified within IMARIS - or other confocal imaging software - in order to assess the cell's environment qualitatively and understand the quantitative outputs from IVEN. Both groups of

'misclassified cells' might then overlap, meaning that cells defining the transition zone could be included in an additional group. It might be worth then to revise the classical nomenclature of 'proximal mural (as opposed to 'distal mural') - Copp [1978] and specify the likely presence of cTE cells within. Even if these 'transition' TE cells - that are in fact cTE - do not physically interact with the ICM, we have demonstrated that IVEN recognizes migrating PE cells as their inside neighbours.

Identification of cavity-adjacent ICM cells

We then aimed to test IVEN's ability to properly recognize the localization of ICM cells in contact with the blastocyst cavity in the same embryos used to test TE classification (Fig. 4A). Such analysis was previously not possible with IVEN and

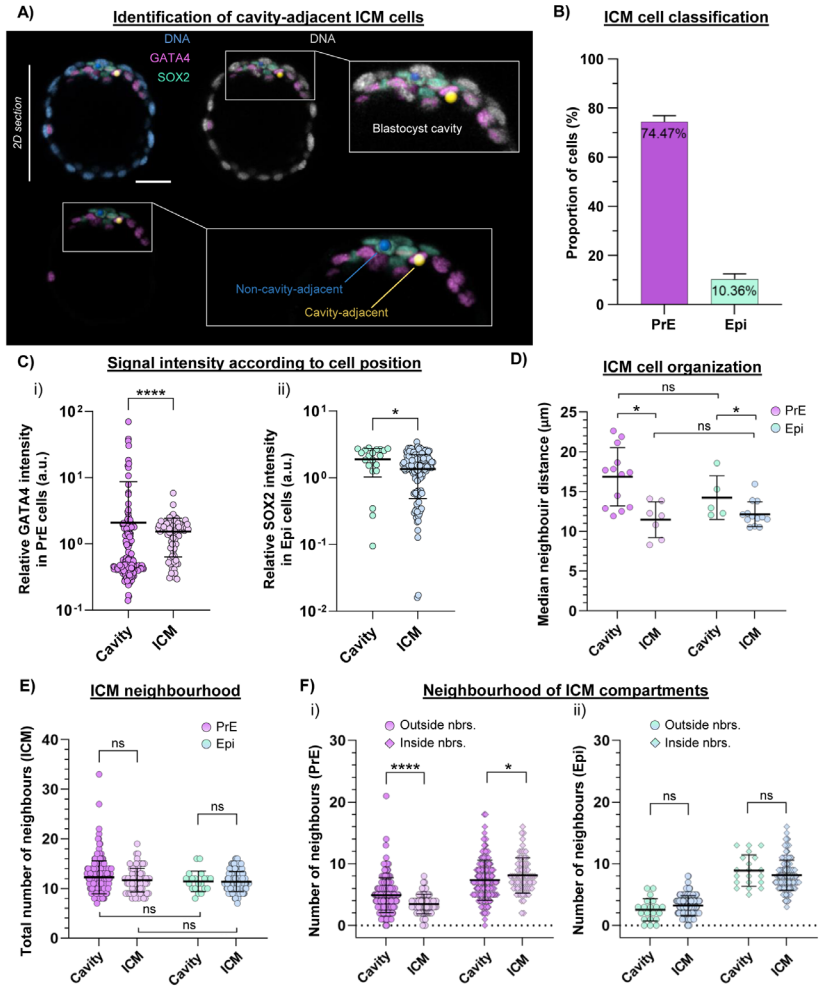

Fig. 4. Characterization of cell subpopulations within ICM lineages according to their position relative to the blastocyst cavity. A) The same blastocyst in Fig. 3F illustrates ICM lineages fully segregated from each other. The inset shows the position of two specific cells detected on IMARIS as classified by IVEN: a PrE cell on the ICM surface correctly identified as adjacent to the cavity (yellow spot), and a cell in the Epi compartment, inside the ICM (blue spot). Scale bar=50 μm. **B)** IVEN´s classification functionality identified 74.47% of the PrE cells as located adjacent to the cavity *versus* 10.36% of the Epi lineage. **C)** Signal intensity of GATA4 and SOX2 in PrE and Epi lineages, respectively, according to cell position (adjacent to the cavity –'cavity'– or fully surrounded by cells –'ICM'). **D)** Distances to neighbours of the same type showed differences between subpopulations of cells from both lineages. Cells embedded in the ICM were shown to display a higher degree of packing when compared to cells from the same lineage in contact with the cavity. **E)** Even though there seemed to be no differences in the overall number of neighbours between groups, **F)** disclosure of cavity *versus* ICM subsets per lineage revealed sensible differences in the neighbourhood composition as regards outside/inside neighbours, in particular for the PrE.

required manual classification via IMARIS. The initial outside/inside classification was confirmed by staining for GATA4 and SOX2 transcription factors as specific markers for the PrE and Epi, respectively. In both lineages, IVEN identified cells as either adjacent or as non-adjacent to the blastocyst cavity; specifically, IVEN classified almost 74.47% of the total PrE cells (identified by the presence of GATA4) in contact with the blastocyst cavity, as opposed to 10.36% of Epi cells from all blastocysts combined (as shown by SOX2 immunostaining) (n_c=475 cells; n_b=13 blastocysts) (Fig. 4B). These results agree with the natural sequence of topological segregation of ICM lineages during blastocyst development. Aiming to identify patterns of transcription factor levels that could explain which cells locate on the surface of the ICM and adjacent to the cavity, we measured signal intensity for GATA4 and SOX2 (Fig. 4C). Our results show much higher values of GATA4 signal for a fraction of cells ($p<0.0001$), and a more spread distribution of values in the cavity-adjacent group than for cells in the ICM (Fig. 4C.i). On the other hand, in this second group values seem to never surpass the threshold marked by the average values of the cavity-adjacent group. These observations might be related to the position of each individual cell on the PrE surface, which could point to a link between transcriptional activity and positional cues for these cells. Parallel analyses of signal values for SOX2 and their position suggested a similar phenomenon; despite the low number of SOX2 cells found on the ICM surface adjacent to the cavity, differences between groups were indeed statistically significant ($p=0.0055$) (Fig. 4C.ii).

According to the median neighbour distance, our data point to different degrees of packing in the organization of cells that are adjacent to the blastocyst cavity when compared to those in the inside of the ICM. Only cells belonging to the same subset within each compartment were considered in one group, i.e., distances were measured between cells in contact with the blastocyst cavity ('cavity-adjacent'), and between cells that are fully embedded in the ICM completely surrounded by cells ('non-cavity-adjacent') ($p=0.0034$ for the comparison within the PrE; $p=0.0460$ for the comparison within the Epi) - Table 2 and Figure 4D. Said differences in cell packing are likely due to the fact that, in E3.5 blastocysts cultured for 24 hours, PrE cells already form an epithelial layer on the surface of the ICM. Epi cells in turn do not organize in

Table 2. Cell environments of ICM lineages from E3.5 blastocysts cultured *in vitro* for 24 hours (I). Subpopulations of cells within ICM lineages display different degree of packing

Blastocysts (n)	ICM lineages	Total cells analyzed	Cavity-adjacent cells	Non-cavity-adjacent cells	Average distance between cavity-adjacent cells (µm)	Average distance between non-cavity-adjacent cells (µm)	Average distance between cells in the lineage (µm)
13	PrE	282	210	72	16.87 (±3.67)	11.46 (±2.25)	15.87 (±3.38)
	Epi	193	20	173	14.24 (±2.75)	12.15 (±1.56)	12.16 (±1.48)

Comparison of the distances between cell centres measured in each compartment/lineage. Results are shown as average ±SD for both the PrE and the Epi lineages, and visible in the plot in Fig. 4D. Mann-Whitney tests for comparison of two non-normally-distributed independent groups were run.

Table 3. Cell environments of ICM lineages from E3.5 blastocysts cultured *in vitro* for 24 hours (II). Characterization of the neighbourhood confirmed specific differences between subsets of PrE cells

Cavity-adjacent cells	Non-cavity-adjacent cells	Average total nbrs. for cavity-adjacent cells	Average total nbrs. for non-cavity-adjacent cells	Average outside nbrs. for cavity-adjacent cells	Average outside nbrs. for non-cavity-adjacent cells	Average inside nbrs. for cavity-adjacent cells	Average inside nbrs. for non-cavity-adjacent cells
210	72	12.27 (±3.33)	11.68 (±2.36)	4.93 (±2.82)	3.49 (±1.60)	7.35 (±3.24)	8.13 (±2.86)
	173	11.45 (±2.06)	11.40 (±2.00)	2.55 (±1.82)	3.24 (±1.60)	8.90 (±2.55)	8.16 (±2.45)

Comparison of the number of neighbours for cavity-adjacent and non-cavity-adjacent cells. Values are shown as average ±SD, and results are plotted in Fig. 4E-F. Mann-Whitney tests for comparison of two non-normally-distributed independent groups were run (n=13 blastocysts).

the same way; however, our results show that these cells might also be subjected to higher compaction when embedded in the ICM than when still in contact with the cavity, which would justify the minor differences observed (Fig. 4D). It is tempting to speculate that cells on the layer adjacent to the cavity are subjected to higher degree of warping movements, mostly due the recurrent compaction and expansion events of the

blastocyst, which could explain the longer distance between centres within these cell groups. Deforming movements during blastocyst maturation are commonly seeing to stretch the cavity-adjacent ICM cells, which occasionally establish physical contact with the TE. Such phenomena have been proposed as a mechanism to facilitate PrE delamination and subsequent PE cell migration [Filimonow and de la Fuente 2022].

We did not find differences in the total number of neighbouring cells between the PrE and the Epi lineages ($p=0.3819$ and $p=0.4184$, for cavity-adjacent and non-cavity-adjacent cells, respectively), nor did our results reveal differences between cells facing the cavity and those inside the ICM ($p=0.3343$ and $p=0.8464$ for cell groups within the PrE and the Epi, respectively) - Table 3 and Figure 4E. To unmask any potentially-hidden connection to neighbour classification, we identified outside and inside cells within both PrE and Epi for each lineage and their subpopulations (cavity *versus* not cavity - ICM), and addressed direct comparisons again. Results are presented as averages per cell (Tab. 3) and as absolute numbers (Fig. 4F.i) In this case, PrE cells in contact with the blastocyst cavity, i.e., fully segregated from the Epi, displayed a higher number of outside neighbours than PrE cells still embedded in the ICM ($p<0.0001$), which in turn seemed to be surrounded by a slightly higher number of inside neighbours ($p=0.0325$) (Fig. 4F.i). Cells from the Epi compartment did not show any differences regarding the number or classification of their neighbours between the cavity-adjacent group and the ICM-contained group ($p=0.0799$ and $p=0.2299$ for outside and inside neighbours, respectively); then again, the low number of cells adjacent to the cavity in this lineage might pose a hindrance for the proper comparison, even when the appropriate test for small size samples was performed (Tab. 3 and Fig. 4F.ii).

Conclusions

The combined use of image analysis software such as IMARIS and IVEN facilitates the discrimination between both cell compartments within the early blastocyst. The updated IVEN version enables the identification of the position of individual cells relative to the blastocyst cavity. The result is a novel approach for the analyses of cell dynamics and blastocyst architecture with particular reference to the cavity. New insights on cell positioning within the ICM uncover differences in compaction but similarities in the organization patterns between PrE and Epi cells, especially considering whether they are fully segregated in the ICM. The original version of IVEN was able to classify the mTE and pTE, however this approach seemingly had limited accuracy in more complex regions of the embryo. The updated approach to identify cavity-adjacent cells (including ICM boundary cells) exhibits improved accuracy and functionality, facilitating further analysis of the border ICM cells and potentially migrating PE cells at the peri-implantation stage. However, to some degree this analysis may be limited by the user's familiarity with the segmentation of the cavity into enough smaller fractions via the GUI. IVEN does indeed classify ICM cells as cavity/non-cavity-adjacent with accuracy, as shown in our analyses. IVEN's

efficiency opens the avenue to prospective studies on additional systems that entail intrinsic scientific and applied interests, such as rabbit, bovine or porcine embryos. Moreover, the potential of IVEN can be used on analyses of other biological hollow structures like tubular or glandular lumens, which will bring a whole new perspective to structural analyses.

Acknowledgements

The authors wish to thank Dr. Berenika Plusa for her insights and helpful discussions of the analyses presented in this study. R.d.l.F. was supported by NCN 2021/05/X/NZ3/00704.

REFERENCES

1. BORLAND R.M., BIGGERS J.D., LECHENE C.P., 1977 – Studies on the composition and formation of mouse blastocoele fluid using electron probe microanalysis. ***Developmental Biology*** 55, 1-8.
2. CHAZAUD C., YAMANAKA Y., PAWSON T., ROSSANT J., 2006 – Early lineage segregation between epiblast and primitive endoderm in mouse blastocysts through the grb2-MAPK pathway. ***Developmental Cell*** 10, 615-624.
3. CHRISTODOULOU N., WEBERLING A., STRATHDEE D., ANDERSON K.I., TIMPSON P., ZERNICKA-GOETZ M., 2019 – Morphogenesis of extra-embryonic tissues directs the remodeling of the mouse embryo at implantation. ***Nature Communications*** 10, 3557.
4. COPP A.J., 1978 – Interaction between inner cell mass and trophectoderm of the mouse blastocyst. I. A study of cellular proliferation. ***Journal of Embryology and Experimental Morphology*** 48, 109-125.
5. DE MOT L., GONZE D, BESSONARD S., CHAZAUD C., GOLDBETER A., DUPONT G., 2016 – Cell fate specification based on tristability in the inner cell mass of mouse blastocysts. ***Biophysics Journal*** 110, 710-722.
6. FILIMONOW K., DE LA FUENTE R., 2022 – Specification and role of extraembryonic endoderm lineages in the periimplantation mouse embryo. ***Theriogenology*** 180, 189-206.
7. FILIMONOW K., SAIZ N., SUWIŃSKA A., WYSZOMIRSKI T., GRABAREK J.B., FERRETTI E., PILISZEK A., PLUSA B., MALESZEWSKI M., 2019 – No evidence of involvement of E-cadherin in cell fate specification or the segregation of Epi and PrE in mouse blastocysts. ***PLoS One*** 14, e0212109.
8. FISCHER S.C., CORUJO-SIMON E., LILAO-GARZON J., STELZER E.H.K., MUÑOZ-DESCALZO S., 2020 – The transition from local to global patterns governs the differentiation of mouse blastocysts. ***PLoS ONE*** 15, e0233030.
9. FORSYTH J.E., AL-ANBAKI A.H., DE LA FUENTE R., MODARE N., PEREZ-CORTES D., RIVERA I., KELLY R.S., COTTER S., PLUSA B., 2021 – IVEN: A quantitative tool to describe 3D cell position and neighbourhood reveals architectural changes in FGF4-treated preimplantation embryos**.** ***PLoS Biology*** 7, e3001345.
10. FULTON B.P., WHITTINGHAM D.G., 1978 – Activation of mammalian oocytes by intracellular injection of calcium. ***Nature*** 273, 149-151.
11. GRABAREK J.B., PLUSA B., 2012 – Live imaging of primitive endoderm precursors in the mouse blastocyst. ***Methods in Molecular Biology*** 916, 275-285.
12. LOU X., KANG M., XENOPOULOS P., MUNOZ-DESCALZO S., HADJANTONAKIS A.K., 2014 – A rapid and efficient 2D/3D nuclear segmentation method for analysis of early mouse embryo and stem cell image data. ***Stem Cell Reports*** 2, 382-397.

13. MANEJWALA F.M., CRAGOE JR. E.J., SCHULTZ R.M., 1989 – Blastocoel expansion in the preimplantation mouse embryo: role of extracellular sodium and chloride and possible apical routes of their entry. ***Developmental Cell*** 133, 210-220.
14. MCLAREN A., SMITH R., 1977 – Functional test of tight junctions in the mouse blastocyst. ***Nature*** 267, 351-353.
15. NICOLSON G.L., YANAGIMACHI R., YANAGIMACHI H., 1975 – Ultrastructural lozalization of lectin-binding sites on the zonae pellucidae and plasma membranes of mammalian eggs. ***Journal of Cell Biology*** 66, 263-274.
16. NISHIOKA N., INOUE K., ADACHI K., KIYONARI H., OTA M., RALSTON A., YABUTA N., HIRAHARA S., STEPHENSON R.O., OGONUKI N., MAKITA R., KURIHARA H., MORIN-KENSICKI E.M., NOJIMA H., ROSSANT J., NAKAO K., NIWA H., SASAKI H., 2009 – The Hippo signaling pathway components Lats and Yap pattern Tead4 activity to distinguish mouse trophectoderm from inner cell mass. ***Developmental Cell*** 16, 398-410.
17. NIWA H., TOYOOKA Y., SHIMOSATO D., STRUMPF D., TAKAHASHI K., YAGI R., ROSSANT J., 2005 – Interaction between Oct3/3 and Cdx2 determines trophectoderm differentiation. ***Cell*** 123, 917-929.
18. PLUSA B., PILISZEK A., FRANKENBERG S., ARTUS J., HADJANTONAKIS A.K., 2008 – Distinct sequential cell behaviours direct primitive endoderm formation in the mouse blastocyst. ***Development*** 135, 3081-3091.
19. RAINA D., BAHADORI A. STANOEV A., PROTZEK M., KOSESKA . SCHRÖTER C., 2021 – Cell-cell communication through FGF4 generates and maintains robust proportions of differentiated cell types in embryonic stem cells. ***Development*** 148, dev.199926.
20. SAIZ N., GRABAREK J.B., SABHERWAL N., PAPALOPULU N., PLUSA B., 2013 – Atypical protein kinase C couples cell sorting with primitive endoderm maturation in the mouse blastocyst. ***Development*** 140, 4311-4322.
21. SAIZ N., MORA-BITRIA L., RAHMAN S., GEORGE H., HERDER J., GARCIA-OJALVO J., HADJANTONAKIS A.K., 2020 – Growth-factor-mediated coupling between lineage size and cell fate choice underlies robustness of mammalian development. ***eLife*** 9, e56079.
22. SAIZ N., WILLIAMS K.M., SESHAN V.E., HADJANTONAKIS A.K., 2016 – Asynchronous fate decisions by single cells collectively ensure consistent lineage composition in the mouse blastocyst. ***Nature Communications*** 7, 13463.
23. SCHLIFFKA M.F., DUMORTIER J.G., PELZER D., MUKHERJEE A., MAÎTRE J.J., 2024 – Inverse blebs operate as hydraulic pumps during mouse blastocyst formation. ***Nature Cell Biology*** doi: 10,1038/s41556-024-01501-z.
24. STRAWBRIDGE S.E., KUROWSKI A., CORUJO-SIMON E., FLETCHER A.N., NICHOLS J., FLETCHER A.G., 2023 – insideOutside: an accessible algorithm for classifying interior and exterior points, with applications in embryology. ***Biology Open*** 12, bio060055.
25. STRUMPF D., MAO C.A., YAMANAKA Y., RALSTON A., CHAWENGSAKSOPHAK K., BECK F., ROSSANT J., 2005 – Cdx2 is required for correct cell fate specification and differentiation of trophectoderm in the mouse blastocyst. ***Development*** 132, 2093-2102.
26. SUTHERLAND A.E., SPEED T.P., Calarco P.G., 1990 – Inner cell allocation in the mouse morula: the role of oriented division during fourth cleavage. ***Developmental Biology*** 137, 13-25.
27. TOSENBERG A., GONZE D., BESSONARD S., COHEN-TANNOUDJI M., CHAZAUD C., CUPONT G., 2017 – A multiscale model of early cell lineage specification including cell division. ***NPJ Systems Biology and Applications*** 3, 16.

28. VELTMAAT J.M., ORELIO C.C., WARD-VAN OOSTWAARD D., VAN ROOIJEN M.A., MUMMERY C.L., DEFIZE L.H., 2000 – Snail is an intermediate early target gene of parathyroid hormone related peptide signaling in parietal endoderm formation. ***The International Journal of Developmental Biology*** 44, 297-307.
29. WILEY L.M., 1984 – Cavitation in the mouse preimplantation embryo: Na/K-ATPase and the origin of nascent blastocoele fluid. ***Developmental Biology*** 105, 330-342.
30. YAMANAKA Y., RALSTON A., STEPHENSON R.O., ROSSANT J., 2006 – Cell and molecular regulation of the mouse blastocyst. ***Developmental Dynamics*** 235, 2301-2314.
31. YANAGIDA A., CORUJO-SIMON E., REVELL C.K., SAHU P., STIRPARO G.G., ASPALTER I.M., WINKEL A.K., PETERS R., DE BELLY H., CASSANI D.A.D., ACHOURI S., BLUMENFELD R., FRANZE K., HANNEZO E., PALUCH E.K., NICHOLS J., CHALUT K.J., 2022 – Cell surface fluctuations regulate early embryonic lineage sorting. ***Cell*** 185, 1258